ACS Medicinal Chemistry Letters

pubs.acs.org/acsmedchemlett Letter

Discovery of a Highly Selective and Potent TRPC3 Inhibitor with High Metabolic Stability and Low Toxicity

Sicheng Zhang,[▽] Luis O. Romero,[▽] Shanshan Deng, Jiaxing Wang, Yong Li, Lei Yang, David J. Hamilton, Duane D. Miller, Francesca-Fang Liao, Julio F. Cordero-Morales,* Zhongzhi Wu,* and Wei Li*

Cite This: *ACS Med. Chem. Lett.* 2021, 12, 572−578 Read Online

ACCESS | Metrics & More | Article Recommendations | Supporting Information

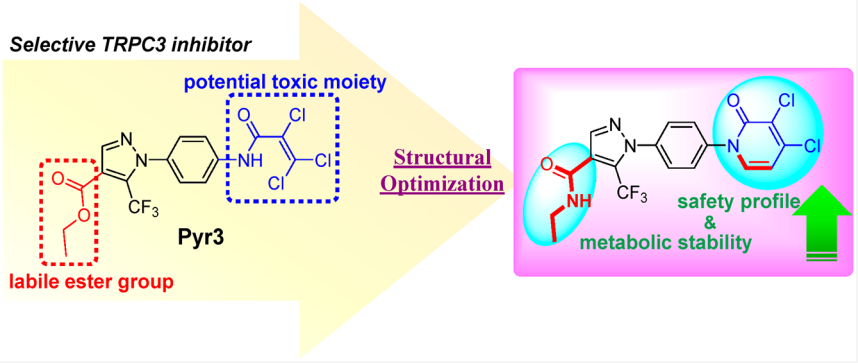

ABSTRACT: The overactivation of transient receptor potential canonical 3 (TRPC3) is associated with neurodegenerative diseases and hypertension. Pyrazole 3 (Pyr3) is reported as the most selective TRPC3 inhibitor, but it has two inherent structural limitations: (1) the labile ester moiety leads to its rapid hydrolysis to the inactive Pyr8 *in vivo*, and (2) the alkylating trichloroacrylic amide moiety is known to be toxic. To circumvent these limitations, we designed a series of conformationally restricted Pyr3 analogues and reported that compound **20** maintains high potency and selectivity for human TRPC3 over its closely related TRP channels. It has significantly improved metabolic stability compared with Pyr3 and has a good safety profile. Preliminary evaluation of **20** demonstrated its ability to rescue Aβ-induced neuron damage with similar potency to that of Pyr3 *in vitro*. Collectively, these results suggest that **20** represents a promising scaffold to potentially ameliorate the symptoms associated with TRPC3-mediated neurological and cardiovascular disorders.

KEYWORDS: *transient receptor potential canonical 3, pyrazole 3, selective inhibitor, high metabolic stability, low toxicity*

Transient receptor potential canonical (TRPC) channels are ubiquitously expressed in vertebrate cells.[1] The TRPC channel subfamily consists of seven members designated as TRPC1−7. Except for pseudogene TRPC2, the other channels are further divided into two groups, TRPC1/4/5 and TRPC3/6/7, based on amino acid sequence homology and functional similarities.[2] As nonselective cationic channels, they control the influx of Ca^{2+} and other cations like Na^{+} in response to activation of phospholipase C-coupled plasma membrane receptors and thus play critical roles in the regulation of intracellular Ca^{2+} concentration by hormones and growth factors.[3,4] Among the TRPC family, TRPC3 plays a prominent functional role in basic cellular responses including proliferation, differentiation, and death in response to various environmental stimuli,[5−7] implying a variety of diverse biological functions.[3] TRPC3 is the most abundant TRPC channel in the brain.[8] Recent studies have suggested that TRPC3 channels are critical for the signaling cascade of brain-derived neurotrophic factors,[9,10] which has been postulated as a critical contributor to Alzheimer's disease.[11] TRPC3 is also expressed in cardiomyocytes, and its overexpression has been found to be involved in adverse stress responses, hypertrophy, and heart failure.[12] In the immune system, it has been suggested to contribute to the restoration of Ca^{2+} influx and activation of T-cells, facilitating the response to antigen stimulation.[13,14] Additionally, TRPC3 is involved in the proliferation and migration of a variety of tumor cells including melanoma, lung, and breast cancers.[15−17]

Current understanding of the role of TRPC3 in pathological studies suggests that selective TRPC3 channel inhibitors may be suitable for the treatment of diseases.[15,18] Over the past

Received: November 2, 2020
Accepted: February 26, 2021
Published: March 5, 2021

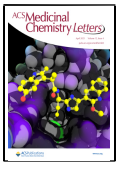

https://dx.doi.org/10.1021/acsmedchemlett.0c00571
ACS Med. Chem. Lett. 2021, 12, 572−578

decade, several TRPC3 inhibitors have been reported and are summarized in Figure 1. Among these inhibitors, Pyr3 is the most selective for TRPC3 inhibition, with a reported IC_{50} value of 0.7 μM, since most of the other inhibitors possess comparable or higher potency against both TRPC3 and TRPC6.[19] Pyr3 has been reported in several pharmacological studies for the treatment of TRPC3-related diseases such as cardiac hypertrophy[19] and smooth muscle proliferation.[18]

However, Pyr3 has two structural liabilities. First, while structure−activity relationship (SAR) studies showed that the trichloroacrylic amide group in Pyr3 (tail moiety in Figure 2) is critical for its TRPC3 inhibition specificity,[20] it is a reactive group with high toxic liabilities. Second, the ester head moiety in Pyr3 can be quickly hydrolyzed *in vivo*, leading to the inactive acid derivative Pyr8.[21] To circumvent these two structural limitations, we hypothesized that incorporating the tail group in a conformationally restricted ring will significantly reduce the alkylating toxicity, and isosterically replacing the ester with a stable linker will improve the metabolic stability. Toward this direction, we designed and synthesized a series of modified pyrazoles as illustrated in Figure 2. Among these molecules, compound **20** shows a significantly improved metabolic stability and safety profile, while maintaining high potency and selectivity for TRPC3 inhibition similar to that of Pyr3. Preliminary evaluation of compound **20** demonstrated its ability to rescue Aβ-induced neuron damages with similar potency to Pyr3.

As the first step of modification, we only replaced the tail moiety with a 6-membered pyridone ring while keeping the rest of the Pyr3 structure intact, to determine whether restricting the conformation in the tail region still maintains TRPC3 inhibition activity at all. To synthesize compounds **2**−**8**, we started from the condensation of ethyl-2-(ethoxymethylene)-4,4,4-trifluoro-3-oxobutanoate and 4-bromophenylhydrazine hydrochloride to produce the pyrazole intermediate **1**. Coupling of **1** with 4-chloropyridone or pyridone afforded **2** or **3**, respectively (Scheme 1a). Treatment of **2** with *N*-chlorosuccinimide (NCS) gave the multichlorinated compounds **4**−**6** (Scheme 1b). Finally, 3,5-dichlorinated **7** and 5-chlorinated **8** were obtained using copper catalyst mediated coupling reactions as shown in Scheme 1c.

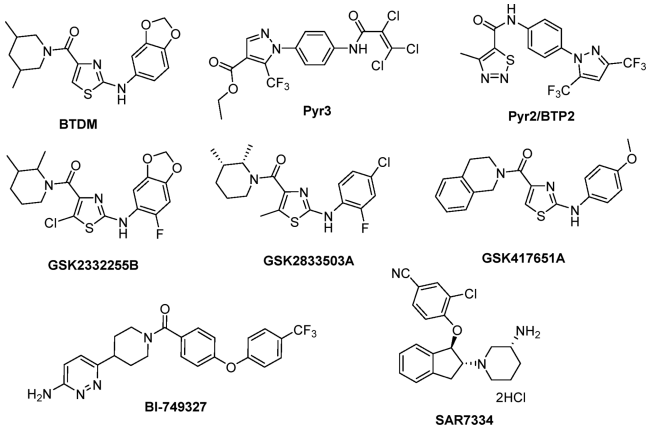

Figure 1. Chemical structures of reported TRPC3 inhibitors.

To make compounds **9** and **10**, fluorine or dibromine was incorporated to compound **2** by the treatment with selectfluor or *N*-bromosuccinimide, respectively (Scheme 2a and b). The corresponding carboxylic acids **11**−**16** were obtained through hydrolysis of the parent ester compounds before they were converted to their corresponding amides **17**−**22** (Scheme 2c).

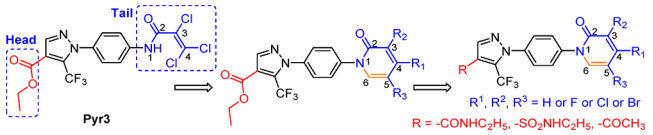

Figure 2. Design of metabolically stable and low toxic selective TRPC3 inhibitors by addressing structural liabilities in Pyr3.

Scheme 1. Synthesis of Ester Compounds 2−8 with Different Chlorine Substitution Patterns[a]

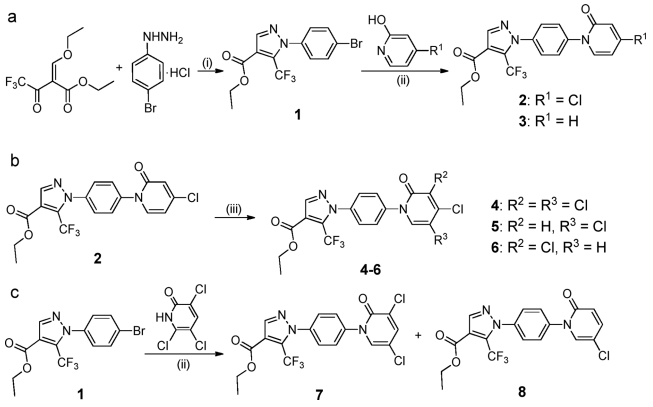

[a]Reagents and conditions: (i) EtOH, 60 °C, 6 h; (ii) CuI, DMCDA, K_2CO_3, toluene, reflux, 12 h; (iii) NCS, DMF, 100 °C, 8 h.

Scheme 2. Synthesis of Amide Compounds 17−22[a]

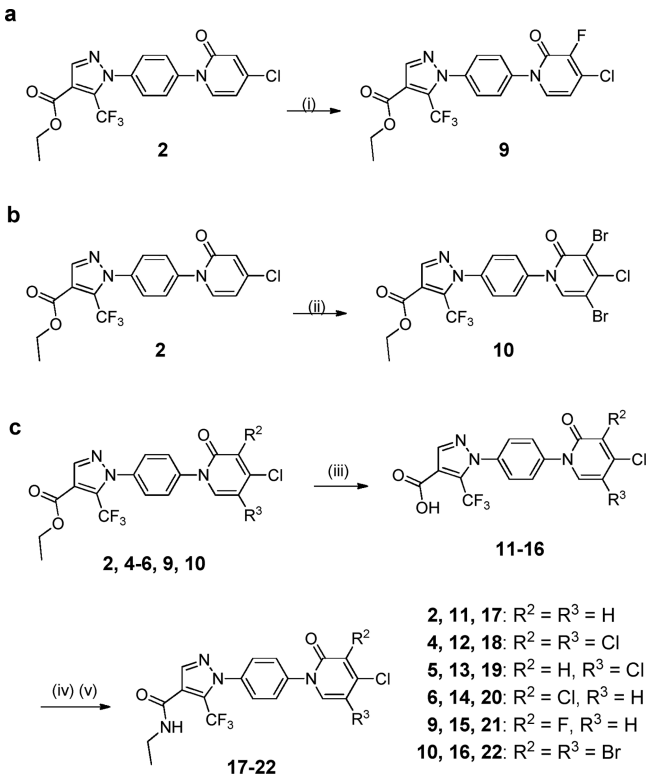

[a]Reagents and conditions: (i) selectfluor, MeCN, 50 °C, 3 h; (ii) NBS, DMF, r.t., 8 h. (iii) 1 M KOH (aq.), EtOH, H_2O, rt, 8 h; (iv) $SOCl_2$, CH_2Cl_2, reflux for 4 h; (v) ethylamine, TEA, r.t., 12 h.

https://dx.doi.org/10.1021/acsmedchemlett.0c00571
ACS Med. Chem. Lett. 2021, 12, 572−578

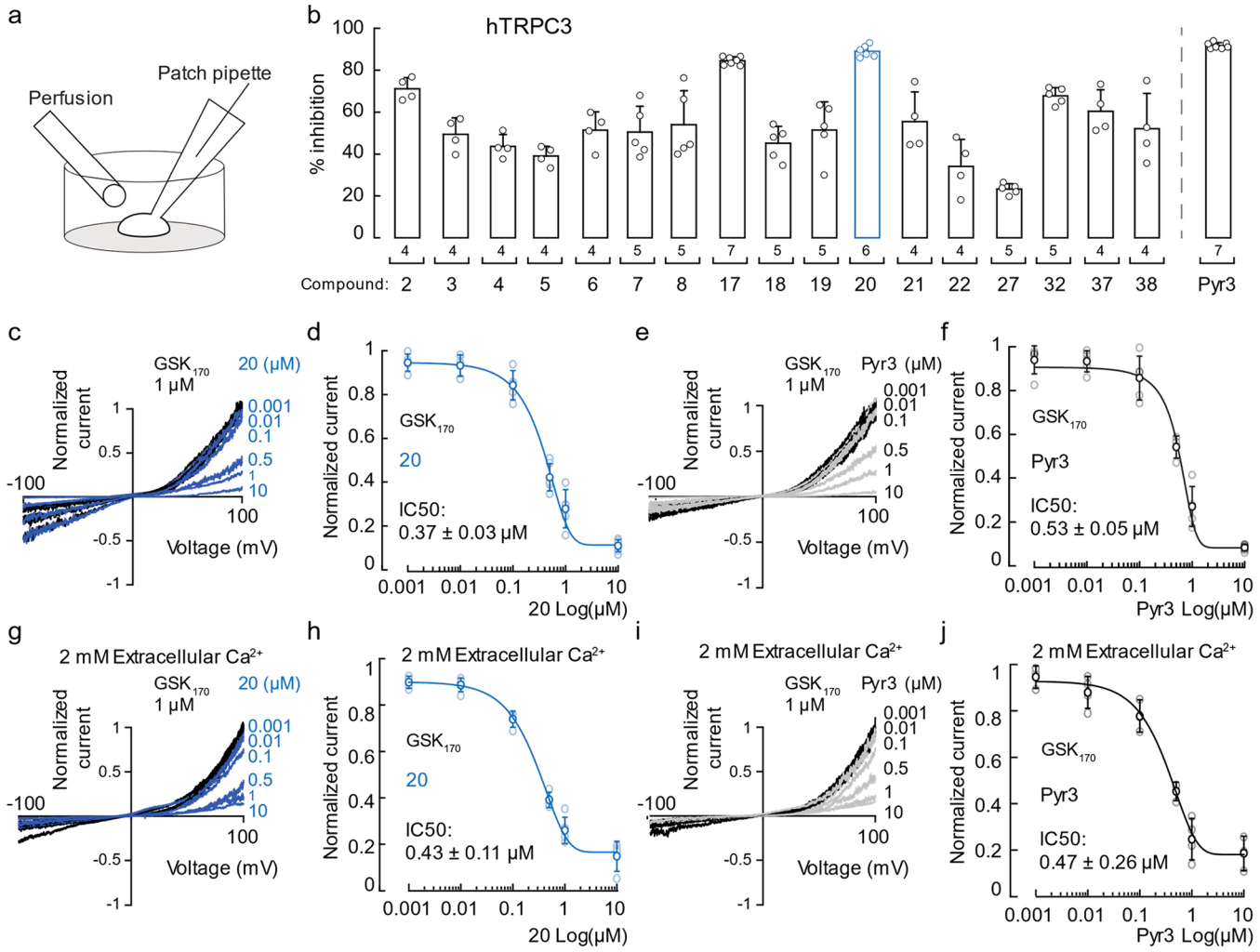

Figure 3. Inhibition of TRPC3-mediated currents by synthesized compounds. (a) Cartoon depicting the experimental conditions used to test the effect of the synthesized compounds on HEK293 cells overexpressing hTRPC3. TRPC3 currents were measured in the whole-cell configuration of the patch-clamp technique, and cells were challenged with agonists/antagonists through perfusion. (b) Percentage of hTRPC3 currents elicited by GSK_{170} and inhibited by the synthesized compounds in transfected HEK293 cells. Bars represent mean ± SD; *n* is denoted above the *x*-axis. (c) Representative traces of hTRPC3 currents activated by 1 μM GSK_{170} and inhibited at different concentrations of compound **20** (blue traces). Each concentration was tested on independent cells and normalized against its internal control (maximum amplitude) to avoid tachyphylaxis. (d) Dose–response profile of hTRPC3 currents elicited by 1 μM GSK_{170} and inhibited at different concentrations of compound **20**. Circles represent mean ± SD. (e) Representative traces of hTRPC3 currents activated by 1 μM GSK_{170} and inhibited at different concentrations of Pyr3 (gray traces). Each concentration was tested on independent cells and normalized against its internal control (maximum amplitude) to avoid tachyphylaxis. (f) Dose–response profile of hTRPC3 currents elicited by 1 μM GSK_{170} and inhibited at different concentrations of Pyr3. Circles represent mean ± SD. (g) Representative traces of hTRPC3 currents activated by 1 μM GSK_{170} and inhibited at different concentrations of compound **20** (blue traces) in the presence of extracellular Ca^{2+} (2 mM). Each concentration was tested on independent cells and normalized against its internal control (maximum amplitude) to avoid tachyphylaxis. (h) Dose–response profile of hTRPC3 currents elicited by 1 μM GSK_{170} and inhibited at different concentrations of compound **20** in the presence of extracellular Ca^{2+} (2 mM). Circles represent mean ± SD. (i) Representative traces of hTRPC3 currents activated by 1 μM GSK_{170} and inhibited at different concentrations of Pyr3 (gray traces) in the presence of extracellular Ca^{2+} (2 mM). Each concentration was tested on independent cells and normalized against its internal control (maximum amplitude) to avoid tachyphylaxis. (j) Dose–response profile of hTRPC3 currents elicited by 1 μM GSK_{170} and inhibited at different concentrations of Pyr3 in the presence of extracellular Ca^{2+} (2 mM). Circles represent mean ± SD. GSK_{170}: GSK1702934A.

Other compounds **27**, **32**, **37**, and **38** were synthesized by following the procedures shown in Supporting Information (Schemes S1–S3). All compounds have purities ≥ 95% based on analytical chemistry characterization (Supporting Information).

We first evaluated the ability of the Pyr3 analogues to inhibit TRPC3 using the patch-clamp technique in the whole-cell configuration (Figure 3a). We activated human TRPC3 (hTRPC3) with a specific agonist, GSK1702934A (GSK_{170}), in HEK293 cells and determined the inhibitory effect of each compound at 10 μM concentration in the presence of the agonist (Figures 3b and S1a). We recorded TRPC3 currents in the absence of Ca^{2+} to evaluate compound inhibition with a minimal contribution of Ca^{2+}-desensitized channels. As expected, Pyr3 inhibited 91 ± 4% (mean ± SD) of hTRPC3 currents. Notably, compound **20** was as efficient as Pyr3 inhibiting hTRPC3 (89 ± 3%), followed by compounds **17** (84 ± 2%) and **2** (71 ± 5%). Further modification of compound **20** by replacing 3-chlorine with 3-fluorine to produce **21** or replacing the amide by a sulfonamide moiety to

https://dx.doi.org/10.1021/acsmedchemlett.0c00571
ACS Med. Chem. Lett. 2021, 12, 572–578

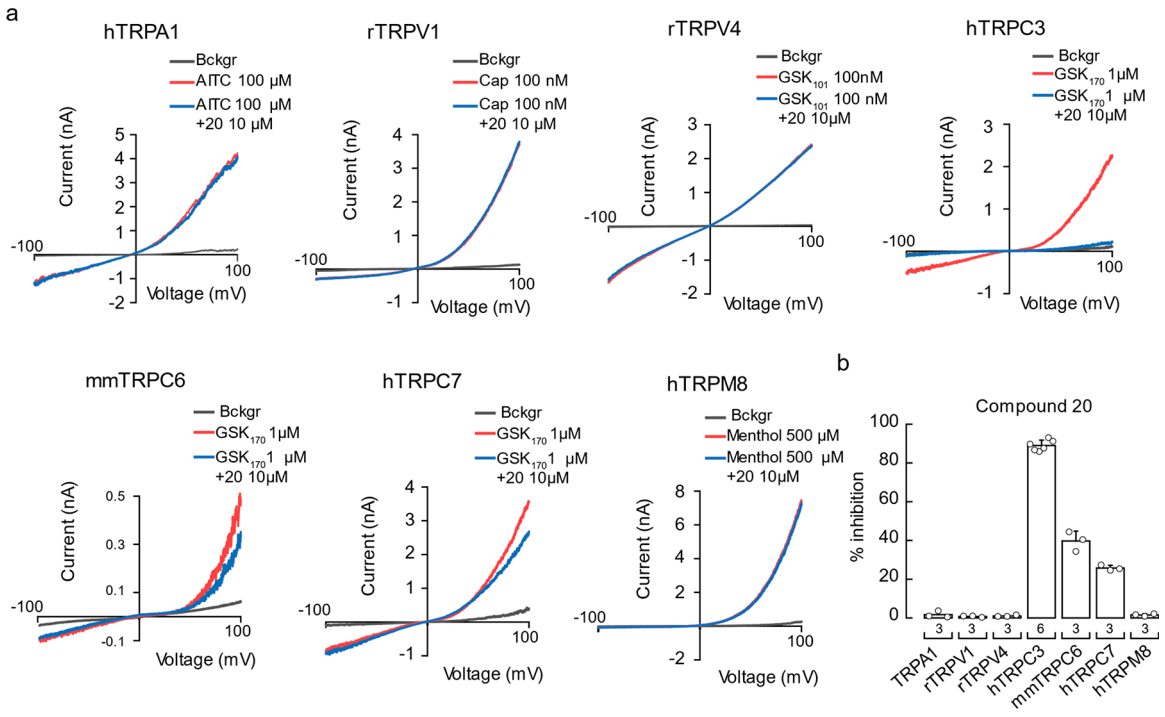

Figure 4. Compound **20** is a selective inhibitor of the TRPC subfamily. (a) Representative whole-cell recordings of HEK293 cells overexpressing hTRPA1, rTRPV1, rTRPV4, hTRPC3, mmTRPC6, hTRPC7, and hTRPM8. Currents were evoked with high concentrations of the agonist (red) and challenged with **20** (10 μM) in the presence of the respective agonist (blue). (b) Percentage of peak current blocked by **20** (10 μM) in the presence of each agonist. AITC, Allyl isothiocyanate; Cap, capsaicin; GSK_{101}, GSK1016790A. Bars are mean ± SD. *n* is denoted above the *x*-axis.

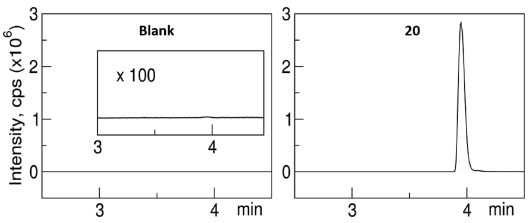

Figure 5. LC/MS analyses of the purified **20**–TRPC3 complexes (right) together with the prepared control (left) support the direct binding of **20** to TRPC3 proteins. Spectra of MS data collected from 2.5 min to avoid buffer salts to MS.

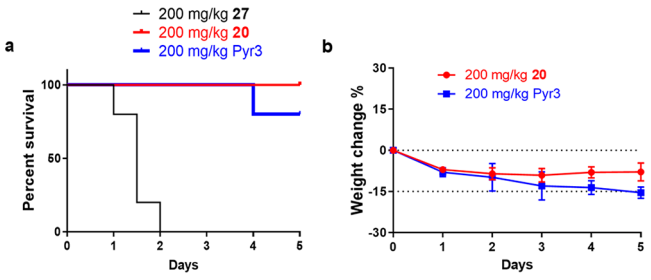

Figure 6. Compound **20** shows a good safety profile in mice. (a) Mouse survival curves. (b) Mean percent change in mouse body weight ± SD relative to body weight at the time of initiating drug treatment. All mice received a daily dose at 200 mg/kg body weight of compounds **20**, **27**, or Pyr3 (n = 5) for 5 consecutive days. Dashed lines indicate mouse weight relative to its respective baseline weight at day 0 and 15% weight loss.

provide **32** failed to further improve the inhibitory potency. Since compound **20** best mimics the structure of Pyr3 (the C5 carbon in compound **20** occupies the position for one of the chlorines at C4 in Pyr3), the overall SAR for this new scaffold is largely consistent with that of the Pyr3 scaffold.[20] It is also interesting to note that the chlorine at C4 in the compound **20** scaffold plays a more important role than the chlorine at C3 or C5, since analogues lacking this C4 chlorine (e.g., **3**, **7**, and **8**) are significantly less potent. As an added benefit, the amide analogues which are predicted to be more metabolically stable also showed higher potency than the corresponding ester analogues (Figure 3b).

Since compound **17** had a slower time course of inhibition than those of Pyr3 and compound **20** (Figure S1b and c), we focused our subsequent studies using compound **20**. We determined the IC_{50} of compound **20** for hTRPC3 inhibition in the absence of extracellular Ca^{2+} as 0.37 ± 0.03 μM (mean ± SD), which is slightly lower than that of Pyr3 (0.53 ± 0.05 μM, Figure 3c–f). We also compared their inhibition potency in the presence of extracellular Ca^{2+} (Figures 3g–j and S2e,f). As expected, **20** showed a comparable potency with Pyr3 at a 2 mM Ca^{2+} concentration. To further confirm the inhibitory activity of compound **20**, we performed a separate experiment with a commonly used TRPC3 agonist, 1-oleoyl-2-acetyl-*sn*-glycerol (OAG, a membrane-permeable analogue of the endogenous agonist diacylglycerol). Compound **20** and Pyr3 showed similar inhibitory effects and a similar trend in the dose–response profile compared to that of GSK_{170} (Figures S1d–f and S2a–d). We next determined the ability of compound **20** to inhibit members of the TRP channel superfamily hTRPA1, rat TRPV1 (rTRPV1), rTRPV4, hTRPC3, mouse TRPC6 (mm TRPC6), hTRPC7, or hTRPM8 overexpressed in HEK293 cells (Figure 4a). The experiments were performed using solutions without Ca^{2+} to avoid TRP channel desensitization.[22] After fully activating these channels with their respective agonists, 10 μM of

https://dx.doi.org/10.1021/acsmedchemlett.0c00571
ACS Med. Chem. Lett. 2021, 12, 572–578

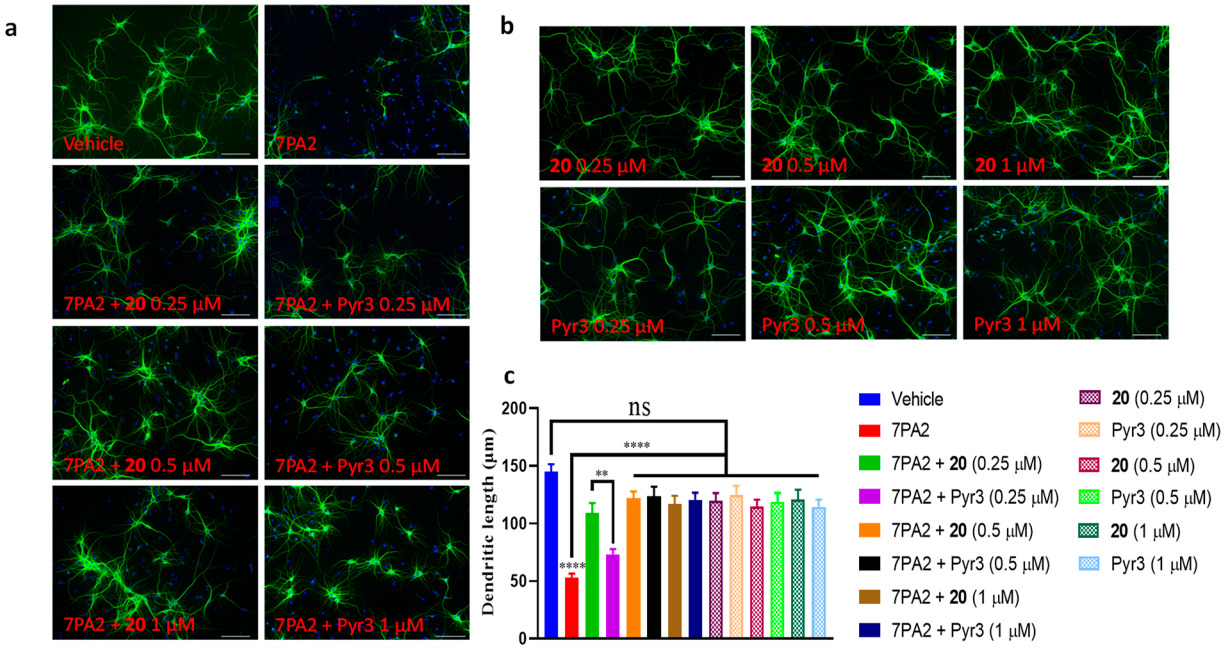

Figure 7. Effects on neuron dendritic morphology. (a) Compound **20** and Pyr3 protect against Aβ-induced damage to dendrites. Mature hippocampal neurons (DIV = 14) were treated with CHO control medium, or naturally secreted Aβ-containing conditioned medium (7PA2)[25] or in combination with compound **20** or Pyr3 at different concentrations, for 16 h, followed by immunocytochemistry using an antibody against MAP2 (green) and DAPI (blue). Scale bar: 100 μm. (b) Lack of toxicity of the inhibitor compounds in neuronal culture. Hippocampal neurons (DIV = 14) were treated with compound **20** or Pyr3 alone at different concentrations, followed by immunocytochemistry staining with MAP2 (green) and DAPI (blue). Scale bar: 100 μm. (c) Quantification of dendritic length. Bars are mean ± SEM. $^{**}p < 0.01$ (one-way ANOVA). $^{****}p < 0.0001$ (one-way ANOVA). $n = 50$ dendrites.

compound **20** was perfused together with the agonists. At this saturating concentration (10 μM), compound **20** failed to inhibit hTRPA1, rTRPV1, rTRPV4, and hTRPM8 currents (Figure 4a and 4b). On the other hand, compound **20** inhibited approximately 39 ± 5% of hTRPC6 and 26 ± 1% of hTRPC7 (Figure 4a and 4b), which are closely related to TRPC3.

Several studies found that Pyr3 inhibits Ca^{2+} release-activated Ca^{2+} channel 1 (Orai1) with comparable blocking potency.[23] Similarly, we found that compound **20** inhibits STIM/Orai mediated Ca^{2+} influx as Pyr3 when activated with thapsigargin (Figure S3). Future modifications could be introduced to compound **20** to discriminate between TRPC3 and STIM/Orai channels. Despite the side effect of pyrazoles at STIM/Orai channels, our results demonstrate that compound **20** is a potent and selective inhibitor of hTRPC3 against other members of the TRP channel superfamily.

To preliminarily confirm the direct on-target engagement of compound **20** with hTRPC3, we performed LC-MS analyses. After incubation of compound **20** with the hTRPC3 protein[2] for 1 h, we performed repeated size-exclusion chromatography to completely remove free compound **20** from the protein-bound fraction. Methanol was then added to this complex to denature the protein and extract the bound compound **20**. As shown in Figure 5, LC-MS detected the presence of compound **20** in the extract solution while no peaks were detected in the control. Since unbound compound **20** was washed out during the complex preparation, this result strongly suggests the direct binding of compound **20** to hTRPC3. Future structural and functional studies with Cryo-EM will reveal the molecular interactions of the complex.

Having confirmed the selective hTRPC3 inhibition and direct molecular interactions, we next evaluated the metabolic stability and safety profile of compound **20**. As expected, the half-life was extended substantially from less than 15 min for Pyr3 to more than 4 h for compound **20** in mouse, rat, and human liver microsomes, consistent with our design to replace the metabolically labile ester headgroup in Pyr3. A preliminary *in vivo* toxicity study was subsequently performed in mice. Because Pyr3 undergoes fast hydrolysis to its inactive metabolite Pyr8 and both showed rapid blood clearance in mice,[21] compound **27**, bearing the same trichloroacrylic amide group as Pyr3 but with a stable amide bond, was used together with Pyr3 as the comparison treatments for the purpose of this toxicity study. All mice ($n = 5$) were treated daily with compounds **20**, **27**, or Pyr3 at 200 mg/kg by intraperitoneal injection for 5 consecutive days, and their survival was monitored. Compound **27** resulted in 100% mortality within 48 h in treated mice. The mice in the Pyr3-treated group with 80% survival dropped by roughly an average of 15% body weight compared to their weights at the start of the experiment, indicating the potential toxicity of Pyr3. In contrast, compound **20** displayed neither mortality nor significant weight loss (Figure 6). Since the only difference between compounds **20** and **27** in structure is their tail moiety, this study provided preliminary evidence that our rational structural modification can significantly decrease the safety liability associated with the trichloroacrylic amide group in Pyr3. It should be noted that since Pyr3 rapidly hydrolyzed *in vivo* to its much polar acid derivative Pyr8 which may have a much faster *in vivo* clearance, the appearance of a lower mortality in Pyr3 treatment group than its metabolically stable analogue **27** is likely due to the fast metabolism and elimination of Pyr3.

Finally, to explore the potential biological effects of **20** in a TRPC3 related disease model, we evaluated its neuroprotective

https://dx.doi.org/10.1021/acsmedchemlett.0c00571
ACS Med. Chem. Lett. 2021, 12, 572−578

ability in primary cultured neurons (14 DIV prepared from E17 rats as described[24]). Compound **20** displayed similar protective effects as Pyr3 in preventing soluble oligomeric Aβ-induced synaptic toxicity on dendritic spine morphology as evidenced by MAP-2 staining (Figure 7).

In summary, we describe here the rational design and preliminary characterization of a new metabolically stable, low-toxic, and selective hTRPC3 inhibitor compound **20**. We also demonstrated the direct binding of compound **20** to hTRPC3 protein and its potential neuroprotective effects. These results indicate that further characterization and optimization of compound **20** may lead to a selective TRPC3 inhibitor as a potentially viable agent for diseases where overexpression of TRPC3 is involved.

■ ASSOCIATED CONTENT

Supporting Information

The Supporting Information is available free of charge at https://pubs.acs.org/doi/10.1021/acsmedchemlett.0c00571.

Whole-cell recording, experimental procedures and methods, characterization data, and ^{1}H and ^{13}C NMR spectra (PDF)

■ AUTHOR INFORMATION

Corresponding Authors

Wei Li − *Department of Pharmaceutical Sciences, College of Pharmacy, the University of Tennessee Health Science Center, Memphis, Tennessee 38163, United States;* orcid.org/0000-0002-9522-4474; Email: wli@uthsc.edu

Zhongzhi Wu − *Department of Pharmaceutical Sciences, College of Pharmacy, the University of Tennessee Health Science Center, Memphis, Tennessee 38163, United States;* Email: jimwu@uthsc.edu

Julio F. Cordero-Morales − *Department of Physiology, the University of Tennessee Health Science Center, Memphis, Tennessee 38163, United States;* Email: jcordero@uthsc.edu

Authors

Sicheng Zhang − *Department of Pharmaceutical Sciences, College of Pharmacy, the University of Tennessee Health Science Center, Memphis, Tennessee 38163, United States;* orcid.org/0000-0003-3798-7550

Luis O. Romero − *Department of Physiology, the University of Tennessee Health Science Center, Memphis, Tennessee 38163, United States; Integrated Biomedical Sciences Graduate Program, College of Graduate Health Sciences, Memphis, Tennessee 38163, United States*

Shanshan Deng − *Department of Pharmaceutical Sciences, College of Pharmacy, the University of Tennessee Health Science Center, Memphis, Tennessee 38163, United States*

Jiaxing Wang − *Department of Pharmaceutical Sciences, College of Pharmacy, the University of Tennessee Health Science Center, Memphis, Tennessee 38163, United States*

Yong Li − *Department of Chemical Biology and Therapeutics, St. Jude Children's Research Hospital, Memphis, Tennessee 38105, United States*

Lei Yang − *Department of Chemical Biology and Therapeutics, St. Jude Children's Research Hospital, Memphis, Tennessee 38105, United States*

David J. Hamilton − *Department of Comparative Medicine, College of Graduate Health Sciences, the University of Tennessee Health Science Center, Memphis, Tennessee 38163, United States*

Duane D. Miller − *Department of Pharmaceutical Sciences, College of Pharmacy, the University of Tennessee Health Science Center, Memphis, Tennessee 38163, United States;* orcid.org/0000-0002-6093-0985

Francesca-Fang Liao − *Department of Pharmacology, Addiction Science, and Toxicology, the University of Tennessee Health Science Center, Memphis, Tennessee 38163, United States*

Complete contact information is available at: https://pubs.acs.org/10.1021/acsmedchemlett.0c00571

Author Contributions

[▽]S.Z. and L.O.R. contributed equally. The manuscript was written through contributions of all authors. All authors have given approval to the final version of the manuscript.

Notes

The authors declare the following competing financial interest(s): W.L., Z.W., and F.L. are listed as inventors for a filed provisional patent application covering these compounds.

■ ACKNOWLEDGMENTS

We thank Dr. Valeria Vásquez and Dr. Lubin Lan (retired) for technical support. We thank Dr. Amanda Clarke at UTHSC for editorial assistance. We thank Dr. Salvatore Mancarella for experimental advice. This work was partially supported by NIH Grants R01GM125629 (to J.F.C.-M.) and R01AG049772 (to F.-F.L.) and funds from a UTHSC CORNET award and the UTCoP Drug Discovery Center (to W.L.). The contents of the article are solely the responsibility of the authors and do not necessarily represent the official views of the NIH.

■ ABBREVIATIONS

AITC, allyl isothiocyanate; Cap, capsaicin; GSK_{101}, GSK1016790A; GSK_{170}, GSK1702934A; NCS, *N*-chlorosuccinimide; OAG, 1-oleoyl-2-acetyl-*sn*-glycerol; Pyr3, pyrazole 3; SAR, structure−activity relationship; TRPC, transient receptor potential canonical.

■ REFERENCES

(1) Venkatachalam, K.; Montell, C. TRP channels. *Annu. Rev. Biochem.* **2007**, *76*, 387−417.

(2) Sierra-Valdez, F.; Azumaya, C. M.; Romero, L. O.; Nakagawa, T.; Cordero-Morales, J. F. Structure-function analyses of the ion channel TRPC3 reveal that its cytoplasmic domain allosterically modulates channel gating. *J. Biol. Chem.* **2018**, *293*, 16102−16114.

(3) Mori, Y.; Wakamori, M.; Miyakawa, T.; Hermosura, M.; Hara, Y.; Nishida, M.; Hirose, K.; Mizushima, A.; Kurosaki, M.; Mori, E.; Gotoh, K.; Okada, T.; Fleig, A.; Penner, R.; Iino, M.; Kurosaki, T. Transient receptor potential 1 regulates capacitative Ca^{2+} entry and Ca^{2+} release from endoplasmic reticulum in B lymphocytes. *J. Exp. Med.* **2002**, *195*, 673−681.

(4) Huang, C. L. The transient receptor potential superfamily of ion channels. *J. Am. Soc. Nephrol.* **2004**, *15*, 1690−1699.

(5) Numaga-Tomita, T.; Oda, S.; Nishiyama, K.; Tanaka, T.; Nishimura, A.; Nishida, M. TRPC channels in exercise-mimetic therapy. *Pfluegers Arch.* **2019**, *471*, 507−517.

(6) Hao, H. B.; Webb, S. E.; Yue, J. B.; Moreau, M.; Leclerc, C.; Miller, A. L. TRPC3 is required for the survival, pluripotency and neural differentiation of mouse embryonic stem cells (mESCs). *Sci. China: Life Sci.* **2018**, *61*, 253−265.

(7) Li, H. S.; Xu, X. Z. S.; Montell, C. Activation of a TRPC3-dependent cation current through the neurotrophin BDNF. *Neuron* **1999**, *24*, 261−273.
(8) Riccio, A.; Medhurst, A. D.; Mattei, C.; Kelsell, R. E.; Calver, A. R.; Randall, A. D.; Benham, C. D.; Pangalos, M. N. mRNA distribution analysis of human TRPC family in CNS and peripheral tissues. *Mol. Brain Res.* **2002**, *109*, 95−104.
(9) Li, Y.; Calfa, G.; Inoue, T.; Amaral, M. D.; Pozzo-Miller, L. Activity-dependent release of endogenous BDNF from mossy fibers evokes a TRPC3 current and Ca^{2+} elevations in CA3 pyramidal neurons. *J. Neurophysiol.* **2010**, *103*, 2846−2856.
(10) Amaral, M. D.; Pozzo-Miller, L. TRPC3 channels are necessary for brain-derived neurotrophic factor to activate a nonselective cationic current and to induce dendritic spine formation. *J. Neurosci.* **2007**, *27*, 5179−5189.
(11) Bathina, S.; Das, U. N. Brain-derived neurotrophic factor and its clinical implications. *Arch. Med. Sci.* **2015**, *6*, 1164−1178.
(12) Bush, E. W.; Hood, D. B.; Papst, P. J.; Chapo, J. A.; Minobe, W.; Bristow, M. R.; Olson, E. N.; McKinsey, T. A. Canonical transient receptor potential channels promote cardiomyocyte hypertrophy through activation of calcineurin signaling. *J. Biol. Chem.* **2006**, *281*, 33487−33496.
(13) Cohen, R.; Torres, A.; Ma, H. T.; Holowka, D.; Baird, B. Ca^{2+} waves initiate antigen-stimulated Ca^{2+} responses in mast cells. *J. Immunol.* **2009**, *183*, 6478−6488.
(14) Philipp, S.; Strauss, B.; Hirnet, D.; Wissenbach, U.; Mery, L.; Flockerzi, V.; Hoth, M. TRPC3 mediates T-cell receptor-dependent calcium entry in human T-lymphocytes. *J. Biol. Chem.* **2003**, *278*, 26629−26638.
(15) Oda, K.; Umemura, M.; Nakakaji, R.; Tanaka, R.; Sato, I.; Nagasako, A.; Oyamada, C.; Baljinnyam, E.; Katsumata, M.; Xie, L. H.; Narikawa, M.; Yamaguchi, Y.; Akimoto, T.; Ohtake, M.; Fujita, T.; Yokoyama, U.; Iwatsubo, K.; Aihara, M.; Ishikawa, Y. Transient receptor potential cation 3 channel regulates melanoma proliferation and migration. *J. Physiol. Sci.* **2017**, *67*, 497−505.
(16) Wang, Y.; Qi, Y. X.; Qi, Z. H.; Tsang, S. Y. TRPC3 regulates the proliferation and apoptosis resistance of triple negative breast cancer cells through the TRPC3/RASA4/MAPK pathway. *Cancers* **2019**, *11*, 558−573.
(17) Aydar, E.; Yeo, S.; Djamgoz, M.; Palmer, C. Abnormal expression, localization and interaction of canonical transient receptor potential ion channels in human breast cancer cell lines and tissues: a potential target for breast cancer diagnosis and therapy. *Cancer Cell Int.* **2009**, *9*, 23−34.
(18) Koenig, S.; Schernthaner, M.; Maechler, H.; Kappe, C. O.; Glasnov, T. N.; Hoefler, G.; Braune, M.; Wittchow, E.; Groschner, K. A TRPC3 blocker, ethyl-1-(4-(2,3,3-trichloroacrylamide)phenyl)-5-(trifluoromethyl)-1H-pyrazole-4-carboxylate (Pyr3), prevents stent-induced arterial remodeling. *J. Pharmacol. Exp. Ther.* **2013**, *344*, 33−40.
(19) Wang, H. B.; Cheng, X. D.; Tian, J. B.; Xiao, Y. L.; Tian, T.; Xu, F. C.; Hong, X. C.; Zhu, M. X. TRPC channels: Structure, function, regulation and recent advances in small molecular probes. *Pharmacol. Ther.* **2020**, *209*, 107497.
(20) Kiyonaka, S.; Kato, K.; Nishida, M.; Mio, K.; Numaga, T.; Sawaguchi, Y.; Yoshida, T.; Wakamori, M.; Mori, E.; Numata, T.; Ishii, M.; Takemoto, H.; Ojida, A.; Watanabe, K.; Uemura, A.; Kurose, H.; Morii, T.; Kobayashi, T.; Sato, Y.; Sato, C.; Hamachi, I.; Mori, Y. Selective and direct inhibition of TRPC3 channels underlies biological activities of a pyrazole compound. *Proc. Natl. Acad. Sci. U. S. A.* **2009**, *106*, 5400−5405.
(21) Hagimori, M.; Murakami, T.; Shimizu, K.; Nishida, M.; Ohshima, T.; Mukai, T. Synthesis of radioiodinated probes to evaluate the biodistribution of a potent TRPC3 inhibitor. *MedChemComm* **2016**, *7*, 1003−1006.
(22) Gordon-Shaag, A.; Zagotta, W. N.; Gordon, S. E. Mechanism of Ca^{2+}-dependent desensitization in TRP channels. *Channels* **2008**, *2*, 125−129.
(23) Schleifer, H.; Doleschal, B.; Lichtenegger, M.; Oppenrieder, R.; Derler, I.; Frischauf, I.; Glasnov, T. N.; Kappe, C. O.; Romanin, C.; Groschner, K. Novel pyrazole compounds for pharmacological discrimination between receptor-operated and store-operated Ca^{2+} entry pathways. *Br. J. Pharmacol.* **2012**, *167*, 1712−1722.
(24) Chen, Y. M.; Wang, B.; Liu, D.; Li, J. J.; Xue, Y. Q.; Sakata, K.; Zhu, L. Q.; Heldt, S. A.; Xu, H. X.; Liao, F. F. Hsp90 chaperone inhibitor 17-AAG attenuates a beta-induced synaptic toxicity and memory impairment. *J. Neurosci.* **2014**, *34*, 2464−2470.
(25) Walsh, D. M.; Klyubin, I.; Fadeeva, J. V.; Cullen, W. K.; Anwyl, R.; Wolfe, M. S.; Rowan, M. J.; Selkoe, D. J. Naturally secreted oligomers of amyloid beta protein potently inhibit hippocampal long-term potentiation in vivo. *Nature* **2002**, *416*, 535−539.

https://dx.doi.org/10.1021/acsmedchemlett.0c00571
ACS Med. Chem. Lett. 2021, 12, 572−578